sustainability

MDPI

Article

Adsorption–Desorption Behaviors of Enrofloxacin and Trimethoprim and Their Interactions with Typical Microplastics in Aqueous Systems

Zhichao Li [1], Xiao Meng [1], Xiaoyong Shi [1,2], Chunyue Li [1,*] and Chuansong Zhang [1,*]

[1] Key Laboratory of Marine Chemistry Theory and Technology, Ministry of Education, Ocean University of China, 238 Songling Road, Qingdao 266100, China; lzc15053719958@163.com (Z.L.); 13935577874@163.com (X.M.); shixy@ouc.edu.cn (X.S.)
[2] National Marine Hazard Mitigation Service, Beijing 100194, China
* Correspondence: lichy1997@163.com (C.L.); zcsong@ouc.edu.cn (C.Z.)

Abstract: Microplastics can transfer antibiotics in water through adsorption and desorption, causing adverse effects on the water environment. Therefore, understanding the interaction between microplastics and antibiotics is important in order to assess their impact on the environment. In this study, the adsorption–desorption behaviors of two commonly used antibiotics [enrofloxacin (ENR) and trimethoprim (TMP)] in aquaculture and their interactions with three typical microplastics [polystyrene (PS), polyvinyl chloride (PVC), and polyethylene (PE)] were investigated through laboratory experiments. The results showed that the adsorption capacity of the three microplastics was 1.229–1.698 mg/g for ENR and 1.110–1.306 mg/g for TMP, correlating with the octanol–water partition coefficients (log K_{ow}) of antibiotics. Due to the larger specific surface areas and special functional groups of microplastics, the antibiotic adsorption capacity of PS and PVC was higher than that of PE. The adsorption behavior followed pseudo-second-order kinetics and a Freundlich isotherm model, indicating a non-uniform surface with multilayer adsorption. A thermodynamic analysis showed that these were all spontaneous endothermic adsorptions. X-ray photoelectron spectroscopy (XPS) and Fourier-transform infrared spectroscopy (FTIR) analyses indicated that the adsorption mechanism was dominated by physical adsorption, involving π–π conjugation, halogen bonds, hydrogen bonding, and electrostatic interactions. High salinity and alkaline environments were conducive to desorption, and the ENR and TMP desorption rates of the microplastics ranged from 20.65% to 24.95%. This indicates that microplastics adsorbed with antibiotics will desorb antibiotics when entering the seawater system, thereby affecting marine ecosystems. These findings reveal the interaction mechanism between microplastics and aquaculture antibiotics in aqueous systems, providing theoretical support for environmental protection and sustainable development.

Keywords: microplastics; antibiotics; adsorption; desorption; environmental protection

Academic Editor: Md. Shahinoor Islam

Received: 5 December 2024
Revised: 28 December 2024
Accepted: 9 January 2025
Published: 10 January 2025

Citation: Li, Z.; Meng, X.; Shi, X.; Li, C.; Zhang, C. Adsorption–Desorption Behaviors of Enrofloxacin and Trimethoprim and Their Interactions with Typical Microplastics in Aqueous Systems. *Sustainability* **2025**, *17*, 516. https://doi.org/10.3390/su17020516

1. Introduction

Since the mid-20th century, enormous quantities of plastic products have been widely used in daily life, leading to increasing plastic pollution in the environment. An estimated 8 million tons of plastics was discharged into the oceans in 2017 [1]. Plastics decompose into small plastic debris of micron or even nanometer size under the combined action of physics, chemistry, and biology [2,3]. Microplastics are plastics characterized by particle sizes smaller than 5 mm [4,5]. Recent studies have shown that microplastics have been

detected in marine water, freshwater, and terrestrial ecosystems [6–11]. The types of microplastics commonly found in the environment include polyethylene (PE), polypropylene (PP), polystyrene (PS), polyvinyl chloride (PVC), polyamide (PA), and polyethylene terephthalate (PET), which account for three-quarters of freshwater microplastic pollution [12,13]. Microplastics can adsorb organic pollutants due to their large specific surface area and strong hydrophobicity in the aquatic environment. As carriers of harmful substances and mixed contamination, microplastics can enter aquatic organisms through ingestion and inhalation, which poses a threat to organisms and human beings due to accumulation in the food chain [14,15]. The high adsorption capacity of microplastics indicates that they are also the source of co-existing organic pollutants [16–18]. Consequently, microplastics have garnered increased attention in scientific research in recent years, primarily due to their perceived risks to aquatic organisms and the environment.

The adsorption of organic pollutants on microplastics has been previously reported [4,19,20]. The adsorption and desorption of organic pollutants on the surface of microplastics is a dynamic process [21], and the adsorption capacity of microplastics is closely related to properties such as their polarity, crystallinity, and specific surface area [19,22]. Velzeboer et al. (2014) reported that microplastics with larger specific surface areas had higher adsorption affinity to organic pollutants [23]. Moreover, the hydrophilicity and hydrophobicity of organic pollutants are important factors affecting the adsorption capacity of microplastics [24].

As a new type of pollutant, antibiotics have attracted increasing attention due to their impact on microbial communities and resistance genes [13,25–28]. China is the leading global producer and consumer of antibiotics. The excessive use of antibiotics has led to a persistent release of these drugs into the environment over the last few decades [29,30]. It has been estimated that approximately 53,800 tons of antibiotics are annually discharged into the aquatic ecosystems in China, and the average concentrations of antibiotics in influent, effluent, and sludge nationwide were 786.2 ng/L, 311.2 ng/L, and 186.8 μg/kg, respectively [31,32]. For example, high concentrations of enrofloxacin (ENR) and trimethoprim (TMP), commonly used in aquaculture, have been detected in the aqueous and solid phases in the Yellow Sea aquaculture zone of the Shandong Peninsula [33]. Once the antibiotics are absorbed by microplastics, they may cause more complex toxicity to aquatic organisms [34,35]. For instance, Lu et al. (2019) found that the absolute abundance of total antibiotic resistance genes on microplastics in aquaculture water is higher than that in water and sediment, affecting bacterial communities in mariculture systems [36]. Li et al. (2018) found that the adsorption coefficient of microplastics to antibiotics correlated positively with the log *Kow* value of antibiotics [34]. Therefore, it is necessary to understand the differences in adsorption behavior and mechanism between microplastics and antibiotics to evaluate their toxicity in the water environment. Furthermore, understanding the thermodynamics of the adsorption process is also important to explain the adsorption mechanism [37,38]. At present, polymer-based photocatalysts have exhibited significant advancements and potential in the removal of antibiotics from water. Polymers' unique properties, ease of modification, and ability to enhance the photocatalytic efficiency of other materials make them promising candidates for sustainable water treatment technologies [39].

Desorption could determine the release degree of organic pollutants from microplastics to environmental media and then affect their environmental migration and bioaccumulation. Organic pollutants that desorb from the surface of microplastics can be absorbed by marine organisms [40]. The negative effects of microplastics on marine organisms have been observed in many studies [41,42]. Hall et al. (2015) found ingested PP in the mesenteric tissue within the coral gut cavity, impeding their digestive function and harming coral

health [43]. As with adsorption, the desorption process is influenced by many factors [44]. As a result, a thorough understanding of the desorption of microplastics and co-existing organic pollutants is very important to fully and precisely elucidate the environmental risks of both.

Environmental factors such as pH, salinity, and aging can affect the adsorption and desorption behaviors of microplastics and antibiotics. Guo et al. (2018) found that the solution pH can alter the ionic forms of microplastics and antibiotics, thereby affecting the adsorption capacity of microplastics [45]. Additionally, high ionic strength may lead to a decrease in adsorption capacity because the presence of high concentrations of ions promotes competition with antibiotics for adsorption sites on the surface of microplastics, thereby inhibiting adsorption. Li et al. (2018) discovered that the adsorption of antibiotics in seawater is significantly lower than in freshwater [34]. However, some studies found that high salinity may inhibit electrostatic interactions, partially neutralizing the negative charge on the surface of microplastics and promoting adsorption behavior [46]. The aging process can cause changes in the physical morphology and chemical properties of microplastics, which also have a significant impact on their adsorption capacity [47,48].

The aim of this study was to understand the mechanisms by which microplastics interact with antibiotics in aquaculture. Therefore, the adsorption kinetics, adsorption isotherm, adsorption thermodynamics and desorption behavior of PS, PVC, and PE microplastics on ENR and TMP were examined. Combined with characterization methods, the adsorption mechanism and the influence of environmental factors on adsorption behavior were analyzed. It was found that the adsorption of ENR and TMP by microplastics was non-uniform multilayer adsorption. The adsorption capacity of ENR on microplastics is higher than that on TMP, and the mechanism is physical adsorption.

2. Materials and Methods

2.1. Materials and Reagents

ENR (≥98%) and TMP (≥98%) were purchased from Shanghai Aladdin Biochemical Technology Co., Ltd. (Shanghai, China) and Shanghai Macklin Biochemical Technology Co., Ltd. (Shanghai, China), respectively. Methanol and acetonitrile were obtained from Merck KGaA (Darmstadt, Germany). All solutions were prepared in ultrapure water obtained from a Milli-Q system (Millipore, Zhangjiagang City, China). PE, PS, and PVC were purchased from Shanghai Yangli Electromechanical Technology Co., Ltd. (Shanghai, China) The particle size of all microplastics was 200 μm.

In order to remove the inorganic salts and oil stains from the surface of the microplastics, the microplastics were immersed in ultra-pure water for 24 h, soaked in 5% HCl for 48 h, and then washed in distilled water, alcohol (analytically pure), and distilled water three times [49]. Finally, the microplastics were transferred into a 50 °C oven for 72 h. After drying, the clean microplastics were stored in a sealable brown vial for use. The zero charge point (PZC) of the microplastics was determined using salt titration [50]. ENR was dissolved in ultrapure water to prepare the stock solutions. Methanol was added to enhance the solubility of TMP in the background solution. To reduce the co-solvent effect, the volume of methanol was controlled below 0.1%. All stock solutions were stored in the refrigerator, away from light, for up to a week.

2.2. Adsorption and Desorption Experiments

An adsorption kinetic experiment was carried out by combining a 20 mg microplastic sample and 30 mL of antibiotics with a concentration of 10 mg/L in 40 mL glass centrifuge tubes. Then, the samples were placed vertically in a water bath thermostatic oscillator (150 r/min, 298 K) in the dark. In the preliminary experiment, samples were collected at 4, 8, 12,

24, 36, 48, 60, and 72 h, and the reaction solution was passed through a 0.22 μm syringe filter for analysis. It was found that adsorption equilibrium could be reached at 48 h. Based on this, the sampling interval was set. At 0.5, 1, 2, 4, 8, 12, 18, 24, 36, and 48 h, the reaction solution was filtered using the same method as the preliminary experiment and then transferred to a 1.5 mL brown chromatographic vial and stored in the dark. For adsorption isotherm experiments, six initial concentrations of antibiotics (2, 5, 10, 15, 20, and 25 mg/L) were selected. The adsorption thermodynamics experiments for the microplastics were carried out at 288 K, 298 K, and 308 K. Under dark conditions at 298 K, the sample solution was filtered at the equilibrium time of 48 h and then loaded into a brown chromatographic vial for detection.

The desorption experiment was carried out after the adsorption experiment. The saturated microplastics were filtered and then dried out. The dried microplastic sample was mixed with 30 mL Milli-Q water in a brown glass vial at 298 K for oscillatory desorption, and the supernatant was filtered for detection after reaching equilibrium for 48 h. The remainder of the process was the same as for the adsorption experiment.

All experiments were performed in triplicate. The adsorption and desorption experiments were carried out at pH = 7.0. Blank adsorption experiments were conducted using a reactor system containing antibiotics without microplastics.

2.3. Effect of Environmental Factors on Adsorption Experiments

In 40 mL glass centrifuge tubes, 20 mg of microplastics was dispersed in 30 mL antibiotics with a concentration of 10 mg/L. The solution pH was adjusted to 3, 5, 7, 9, and 11 using a 0.1 M HCl and 0.1 M NaOH solution to investigate the effect of different pH levels on adsorption. The solution salinity was adjusted to 8.75‰, 17.5‰, 26.25‰, and 35‰ using NaCl solution to study the impact of different salinity levels on adsorption.

Simulated sunlight aging of the microplastics was conducted using a UV lamp in this experiment, with four 15W UV lamps emitting UV light at 254 nm. Pre-treated microplastics were evenly dispersed in Petri dishes and exposed to UV light, with the samples being flipped every 12 h to ensure uniform irradiation. The irradiation experiment lasted a total of 96 h, with aged microplastics collected at 24, 36, 48, 72, and 96 h. Subsequently, 20 mg of aged microplastics was dispersed in 30 mL of antibiotics with a concentration of 10 mg/L in 40 mL glass centrifuge tubes to investigate the effect of aging on adsorption. The sample treatment method was the same as the adsorption isotherm experiment. Under the same conditions, each experiment was repeated three times, and a blank control was set up.

2.4. Characterization of Microplastics and Antibiotic Determination

The surface morphology of the microplastics was characterized via scanning electron microscopy (SEM, Hitachi Ltd., Kanagawa, Japan). The surface area was determined though N2 adsorption desorption with the Brunauer–Emmett–Teller method (BET, Micromeritics Instrument Corp., Norcross, GA, USA). The structure functional groups of the microplastics were characterized using Fourier-transform infrared spectroscopy (FTIR, Thermo Electron Corp., Waltham, MA, USA). The scanning wavenumber of the sample ranged from 4000 to 500 cm^{-1}. The crystalline compositions of the microplastics were measured using an X-ray diffractometer (XRD, Bruker Corp., Karlsruhe, Germany) with a Cu target as the radiation source. The samples were scanned at a rate of 2°/min in the range of 5–90° of 2θ. X-ray photoelectron spectroscopy (XPS, Thermo Electron Corp., Waltham, MA, USA) was performed using a monochromatic Al target (E = 1486.68 eV). A band of 100 eV was used to measure the spectrum, and 20 eV was used for detailed spectra of C 1s, N 1s, and F 1s.

The concentrations of antibiotics were determined via high-performance liquid chromatography (HPLC, Bonna-Agela Technology Co., Ltd., Tianjin, China) coupled with an

Agilent PLRP-S C18 column (4.6 × 250 mm, 5 μm). The mobile phase of ENR was acetonitrile and a 0.2% acetic acid solution with a volume ratio of 25:75. The detection wavelength was 278 nm. For TMP, the mobile phase was acetonitrile and a 1% acetic acid solution at a ratio of 20:80 (v/v), and the detection wavelength was 271 nm. The flow rate was 1.0 mL/min, the injection volume was 20 μL, and the column temperature was maintained at 25 °C.

2.5. Adsorption Model and Data Analysis

The adsorption kinetic data were interpreted using pseudo-first-order and pseudo-second-order models.

Pseudo-first order:

$$\ln(q_e - q_t) = \ln q_e - K_1 t \quad (1)$$

Pseudo-second order:

$$\frac{t}{q_t} = \frac{1}{(K_2 q_e^2)} + \frac{t}{q_e} \quad (2)$$

Here, q_t and q_e (mg/g) are the number of antibiotics adsorbed on the microplastics at a given time t (h) and at equilibrium, respectively. K_1 (1/h) and K_2 (g/mg·h) are the pseudo-first-order kinetic rate constants and pseudo-second-order kinetic rate constants, respectively.

The adsorption isotherms were fitted with Linear, Freundlich, and Langmuir models.

Linear model:

$$q_e = K_d C_e \quad (3)$$

Freundlich model:

$$q_e = K_f C_e^{\frac{1}{n}} \quad (4)$$

Langmuir model:

$$q_e = \frac{K_l q_m C_e}{1 + K_l C_e} \quad (5)$$

where q_e (mg/g) is the adsorption amount of antibiotics on the microplastics; C_e (mg/L) is the equilibrium concentration of antibiotics in the aqueous phase; K_d (L/g) is the partition coefficient; K_f [(mg/g) (L/mg)$^{1/n}$] is the Freundlich adsorption coefficient, indicating the adsorption capacity; 1/n represents the degree of nonlinearity of the adsorption isotherm; q_m (mg/g) is the maximum adsorption capacity of microplastics to antibiotics; and K_l (L/mg) is the Langmuir constant, which is related to the adsorption rate.

The Van't Hoff equation was used to perform the thermodynamic calculations on the adsorption data of antibiotics on microplastics. ΔG^0, ΔH^0, and ΔS^0 were calculated using the following equations:

$$K_d = \frac{q_e}{C_e} \quad (6)$$

$$\Delta G^0 = -RT \ln K_d \quad (7)$$

$$\ln K_d = -\frac{\Delta H^0}{RT} + \frac{\Delta S^0}{R} \quad (8)$$

where K_d (L/g) is the equilibrium constant obtained from the isothermal adsorption model, ΔG^0 (kJ/mol) is the Gibbs free energy, ΔH^0 (kJ/mol) is the enthalpy change, ΔS^0 (J/mol·K) is the entropy change, R (8.314 J/mol·K) is the ideal gas constant, and T (K) is the Kelvin temperature.

SPSS 25.0 software (IBM Corp., Armonk, NY, USA) was used for statistical analysis.

3. Results and Discussion

3.1. Adsorption Behavior Analysis

3.1.1. Adsorption Kinetics

The adsorption kinetics of the antibiotics on the microplastics are shown in Figure 1. The adsorption capacity of the microplastics increased with time. The rate of adsorption of antibiotics by the microplastics was high at first and then slowed. Gupta et al. (2010) proposed that the rate of adsorption is directly proportional to the quantity of vacant sites available [51]. The adsorption process can be described as having three stages: (1) initial rapid adsorption (0–10 h), during which the microplastics exhibited a faster adsorption rate for antibiotics due to a large number of unoccupied sites; (2) a slow adsorption stage (10–36 h), during which the adsorption rate of microplastics to antibiotics tended to be flat due to the gradual occupation of the adsorption sites; and (3) the final equilibrium stage (36–48 h), during which ENR and TMP reached adsorption equilibrium at approximately 36 h and 48 h, respectively.

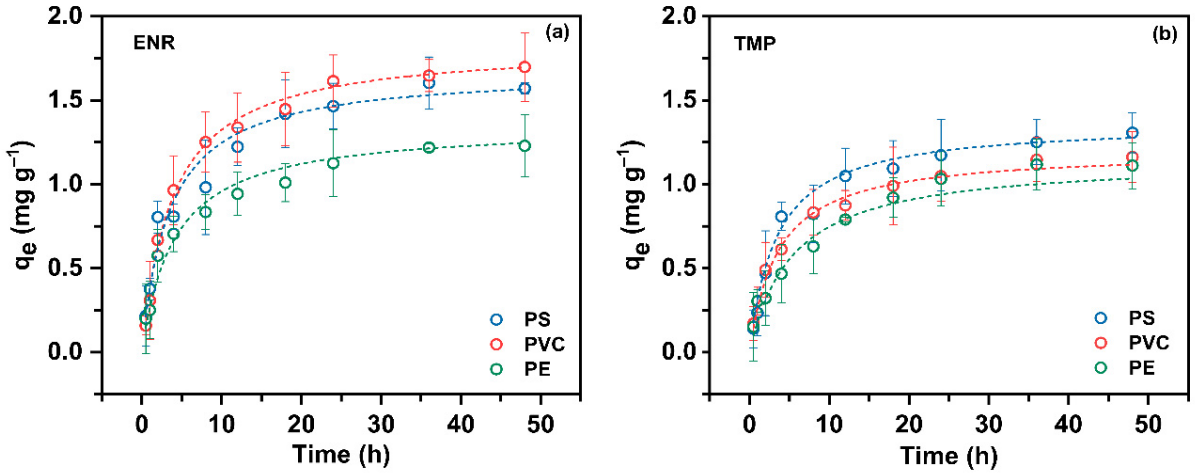

Figure 1. Pseudo-second-order curves of ENR (**a**) and TMP (**b**) on PS, PVC, and PE.

The fitting parameters of the adsorption kinetics model for the microplastic adsorption data are shown in Table 1. Compared with the pseudo-first-order model, the adsorption data were fitted better by the pseudo-second-order model (R^2: 0.934–0.994), and the fitted equilibrium adsorption amount (q_e) was close to the real equilibrium adsorption amount ($q_{e\,exp}$). Zahmatkesh et al. (2023) found that the adsorption of tetracycline by polyvinyl chloride also conforms to the pseudo-second-order model [52]. The results showed that different microplastics have different adsorption capacities for the two antibiotics. The adsorption capacities of PS and PVC on ENR and TMP were significantly higher than those of PE ($p < 0.05$), and the adsorption capacity of three kinds of microplastics on ENR (1.229–1.698 mg/g) was significantly higher than that of TMP (1.110–1.306 mg/g) ($p < 0.05$). The K_2 value of ENR was less than the corresponding K_2 value of TMP, indicating that the adsorption rate decreased with time because the adsorption sites on the surface of the microplastics were rapidly occupied by ENR in the mixed system [53].

As shown in Table 1, the adsorption capacity of three microplastics on ENR was higher than that of TMP. These results imply that the properties of antibiotics can affect their adsorptions on microplastics. Here, the difference in the adsorption behavior of microplastics towards ENR and TMP may be due to the different hydrophobicity of antibiotics. Wu et al. (2016) found that the adsorption process of microplastics was affected by the distribution coefficient of octyl–water (log *Kow*) in the adsorbate [54]. The order of the log *Kow* values of the two antibiotics was as follows: ENR (1.10) > TMP (0.91) [55]. The hydrophobic

interaction between microplastics and ENR is stronger, enhancing the affinity between them, consistent with the order of antibiotic adsorption. Due to the larger molecular weight of ENR compared to TMP, when ENR comes into contact with microplastics, the dispersion force may be stronger, making it easier for ENR to bind to the surface of microplastics.

Table 1. Adsorption kinetic model parameters for antibiotic adsorption on microplastics.

	Pseudo-First Order			Pseudo-Second Order			$q_{e\ exp}$
	K_1 (1/h)	q_e (mg/g)	R^2	K_2 (g/mg·h)	q_e (mg/g)	R^2	
				ENR			
PS	0.222	1.547	0.951	0.172	1.678	0.979	1.570
PVC	0.245	1.604	0.989	0.143	1.831	0.994	1.698
PE	0.173	1.213	0.929	0.180	1.352	0.976	1.229
				TMP			
PS	0.242	1.211	0.957	0.216	1.366	0.976	1.306
PVC	0.231	1.041	0.938	0.232	1.200	0.985	1.162
PE	0.114	1.065	0.881	0.161	1.151	0.934	1.110

$q_{e\ exp}$: Real equilibrium adsorption amount (mg/g) in 48 h.

3.1.2. Adsorption Isotherms

The adsorption isothermal characteristics of different microplastics for the two antibiotics are shown in Figure 2. The antibiotic adsorption capacity of the microplastics increased as the concentration of antibiotics increased, and the adsorption capacity was consistent with the results of the kinetic model.

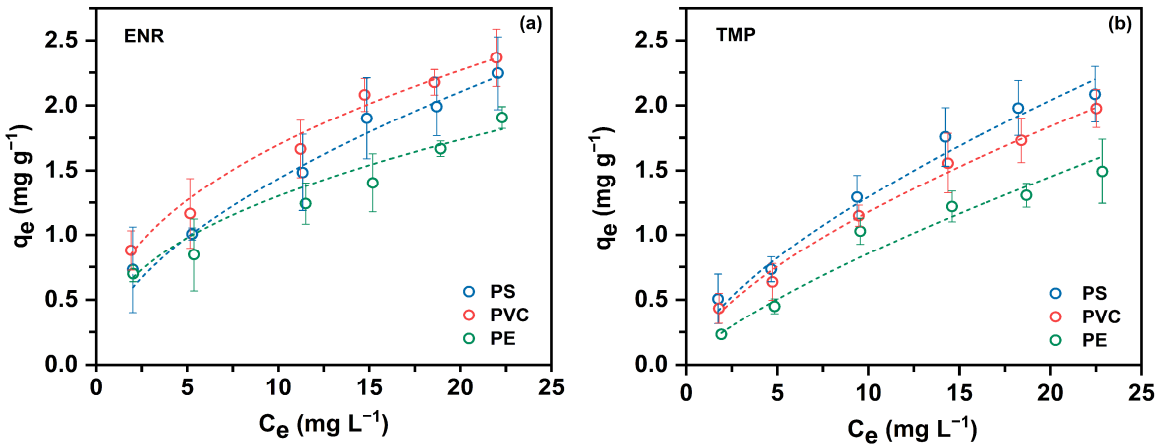

Figure 2. Adsorption isotherms for ENR (**a**) and TMP (**b**) by PS, PVC, and PE.

Many studies found that the linearity of adsorption isotherms varied among chemicals and plastic types [24,56,57]. Therefore, both linear and nonlinear adsorption isotherm models (Freundlich and Langmuir models) were used to fit the experimental data, and the results are summarized in Table 2. For all microplastics, the fitting results clearly showed that the R^2 values of the Freundlich model (0.966~0.991) were large. Thus, the adsorption data were fitted well by the nonlinear Freundlich model, indicating that the adsorption of antibiotics by microplastics was multilayer in nature on non-uniform surfaces [58,59]. Sun et al. (2022) found that the adsorption isotherms of PS and PE for norfloxacin were consistent with the Langmuir model [60]. Consequently, the distribution of adsorption sites and active groups on the surface of all microplastics was uneven, which may have been caused by spherical bulges and cracks on the microplastics [61]. This meant that the high-energy sites of the microplastics were occupied first, followed by lower-energy sites [45,62]. The nonlinear relationship between antibiotic concentration and adsorption

amount indicates that adsorption capacity is not only related to the concentration of antibiotics, but is also affected by other complex factors.

Table 2. Adsorption isotherm model parameters for antibiotic adsorption on microplastics.

Microplastic	Linear		Freundlich			Langmuir		
	K_d (L/g)	R^2	K_f [(mg/g) (L/mg)$^{1/n}$]	1/n	R^2	q_m (mg/g)	K_l (L/mg)	R^2
ENR								
PS	0.145	0.908	0.404	0.551	0.990	3.373	0.081	0.974
PVC	0.124	0.962	0.648	0.419	0.981	2.774	0.195	0.947
PE	0.089	0.942	0.500	0.416	0.979	2.110	0.222	0.938
TMP								
PS	0.112	0.954	0.287	0.655	0.977	4.019	0.051	0.979
PVC	0.100	0.965	0.269	0.642	0.991	3.758	0.048	0.978
PE	0.080	0.958	0.147	0.764	0.966	3.185	0.040	0.977

In this study, all of the 1/n values were lower than 1, indicating preferential adsorption behavior [63]. The K_f values for ENR were higher than those for TMP, suggesting that the adsorption capacity of the microplastics to ENR was higher than TMP. For ENR, PVC showed maximum K_f, while for TMP, PS showed maximum K_f. At the same time, the maximum adsorption capacity of PVC to ENR was 2.774 mg/g, and that of PS to TMP was 4.019 mg/g, which is consistent with the results of adsorption kinetics studies. This further indicates that PVC and PS have stronger adsorption strength and capacity, making them more likely to carry more antibiotics in aquatic environments, especially hydrophobic ENR, and other pollutants, thereby affecting the aquatic behavior of antibiotics and altering their potential ecological risks.

3.1.3. Adsorption Thermodynamics

As can be seen from Figure 3, the adsorption capacity of the two antibiotics on the microplastics increased with the increase in temperature. The interaction between the antibiotics and the adsorption sites was the key factor in determining the adsorption capacity. The increase in the amount of adsorbed antibiotics indicated that the interaction force between the antibiotics and microplastic surface increased at high temperatures [64]. At the same time, following the temperature increases, the molecules diffused more quickly, and the solution became less viscous, making it easier for antibiotic molecules to pass through the outer surface of the microplastic and into the pore structure [65].

To analyze the energy changes involved in the adsorption process, the thermodynamic parameters, standard Gibbs free energy change (ΔG^0), standard enthalpy change (ΔH^0), and standard entropy change (ΔS^0) were calculated, and the results are shown in Table 3. In all of the adsorption systems, the ΔG^0 was negative and ΔH^0 and ΔS^0 were positive, which meant that the adsorption on the microplastics was a spontaneous endothermic reaction [66].

The ΔG^0 of all reaction systems showed a decreasing trend with the increase in temperature, indicating that the driving force of adsorption was stronger at higher temperatures. The results showed that the ΔG^0 of ENR was generally smaller than that of TMP under the same conditions, which indicates that the adsorption of ENR by the microplastics had strong spontaneity. Moreover, the positive ΔH^0 of ENR and TMP adsorption indicated that the process was an endothermic reaction. The results of this study showed that the ΔH^0 in the six adsorption systems was generally less than 40 KJ/mol, indicating that physical adsorption participated in the adsorption process and that hydrogen bonding forces may be involved [37,67,68]. The ΔH^0 values for PVC and PS were higher than that of PE, indicating

that the adsorption process on PVC and PS surfaces was more endothermic [67]. In this experiment, ΔS^0 was positive, which meant that the disorder of the system increased in the adsorption process. Compared with the adsorption system of TMP, the value of ΔS^0 in the adsorption system of ENR was higher. Pan et al. (2012) suggested that, in the adsorption system containing aqueous solutions, the adsorbate destroyed the hydration shell around the active site of the adsorbent, thus increasing the degree of chaos in the system [69]. Chen et al. (2021) suggested that the ΔS^0 value during the adsorption behavior was the result of solute adsorption and solvent desorption in the system [38]. Therefore, it can be inferred that when the ENR and TMP molecules were adsorbed on the microplastic, water molecules were desorbed from the surface of the microplastic, thus intensifying the confusion of the solid–liquid interface.

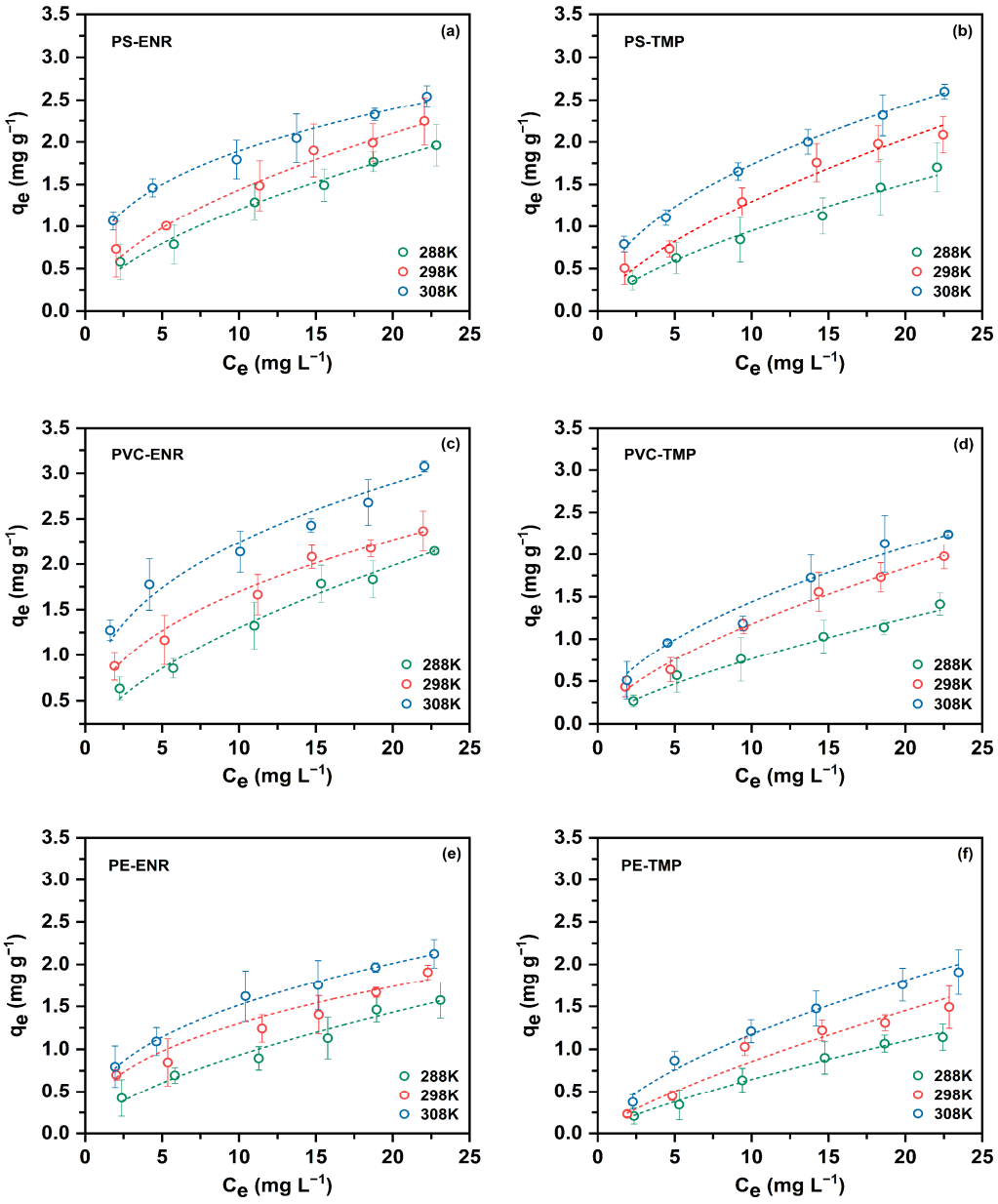

Figure 3. Thermodynamic adsorption curves of PS (**a**,**b**), PVC (**c**,**d**), and PE (**e**,**f**) for ENR and TMP, respectively.

Table 3. Adsorption thermodynamic parameters for antibiotic adsorption on microplastics.

Microplastics	T (K)	lnK_d	ΔG^0 (kJ/mol)	ΔH^0 (kJ/mol)	ΔS^0 (J/mol·K)
			ENR		
PS	288	5.728	−13.714	38.320	179.964
	298	6.002	−14.870		
	308	6.773	−17.343		
PVC	288	5.775	−13.828	40.549	189.443
	298	6.473	−16.038		
	308	6.874	−17.603		
PE	288	5.400	−12.931	36.575	172.713
	298	6.214	−15.397		
	308	6.385	−16.351		
			TMP		
PS	288	5.295	−12.679	37.997	175.503
	298	5.659	−14.020		
	308	6.330	−16.208		
PVC	288	5.017	−12.013	37.675	172.662
	298	5.594	−13.859		
	308	6.038	−15.461		
PE	288	4.707	−11.270	34.364	157.917
	298	4.990	−12.364		
	308	5.643	−14.450		

3.2. Desorption Behavior Analysis

Desorption is one of the basic processes to control the persistence and ecological impact of organic pollutants in aquatic systems [70]. The difference in the rate of desorption of ENR and TMP for three microplastics is shown in Figure 4. In this study, the desorption rates of the three microplastics to ENR were PE > PVC > PS ($p < 0.05$), ranging from 20.65% to 21.88%. The TMP desorption rate of PVC and PE was significantly higher than that of PS ($p < 0.05$), and the TMP desorption rate of PE was the highest, reaching 24.95%. The TMP desorption rate was higher than that of ENR, and the TMP desorption rate of PVC was significantly higher than that of ENR ($p < 0.05$).

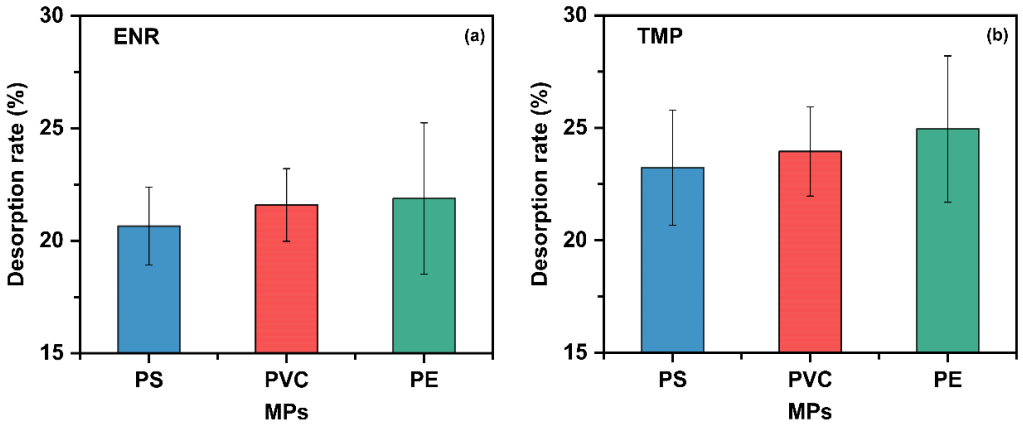

Figure 4. Desorption rates of ENR (**a**) and TMP (**b**) on PS, PVC, and PE.

Desorption behavior is related to the types of microplastics and antibiotics. Through surface normalization analysis, Zuo et al. (2019) found that the desorption behavior of microplastics mainly depends on the abundance of rubbery subfraction [71]. The rubber subfraction ratio of the three microplastics was in the order of PE > PS > PVC [72], indicating that the free volume between the molecular chain segments of PE was larger, and the antibiotics were more easily detached [73,74]. Therefore, the antibiotics adsorbed by PE are easily desorbed, with the highest desorption rate for both antibiotics. Furthermore, the low desorption rate of ENR may be related to hydrophobic interaction. León et al. (2019) found that the average desorption rate of hydrophilic triazine compounds that were not easily adsorbed on microplastics was 85% ± 34%, while hydrophobic PCBs had almost no desorption [75]. This may be due to the strong affinity between hydrophobic organic compounds and the adsorption sites of microplastics, meaning that ENR is not easily detached from the microplastic surface. The desorption results showed that PE had strong desorption potential and released more antibiotics during migration, which can cause harm to the aquatic environment and aquatic organisms.

3.3. Adsorption Mechanisms

3.3.1. Characterization of Microplastics

From Figure 5, it can be observed that the surface of the PVC was slightly rougher than that of the PS and PE. PS microplastics were flaky, and the surface was a network structure with many cracks. The PVC and PE microplastics were pellet-shaped, and irregular cluster aggregation was observed on the surface. The S_{BET} of the PVC (1.357 m^2/g) was larger than that of the PS (0.830 m^2/g) and PE (0.902 m^2/g). The SBET of the PVC was about 1.635 times that of PS and 1.504 times that of PE. Fan et al. (2021) found that the specific surface area of microplastics could increase the size of the adsorption site and enhance the adsorption ability [47]. PVC has the largest specific surface area, with granular protrusions and cracks on the surface, providing more adsorption sites for antibiotics.

As shown in Figure S1, a sharp diffraction peak appeared in the XRD pattern of PE, indicating that PE had a high degree of crystallization. The XRD pattern of PS shows an obvious high intensity peak. For PVC, there is no apparent diffraction peak in the 2θ range of 5–90°. Therefore, the degree of crystallinity followed the order PE > PS > PVC. The XRD patterns of the three microplastics that adsorbed ENR and TMP exhibited no significant change, indicating that the crystallinity of the microplastics before and after the adsorption of ENR and TMP was similar. The pH_{pzc} of PS, PVC, and PE was 4.76, 4.95, and 4.53, respectively. Therefore, under our experimental conditions (pH = 7.0), the microplastics carried net negative charges.

The polarity of microplastics can affect the adsorption capacity. Wang et al. found perfluorooctane sulfonate (PFOS) and perfluorooctane sulfonamide (FOSA) adsorption on microplastics under the influence of microplastic polarity [19]. Both ENR and TMP are polar antibiotics. The results showed that the amount of antibiotics adsorbed by non-polar PE was low (ENR: 1.229 mg/g, TMP: 1.110 mg/g), while the amount of antibiotics adsorbed by polar PVC was high (ENR: 1.698 mg/g, TMP: 1.162 mg/g).

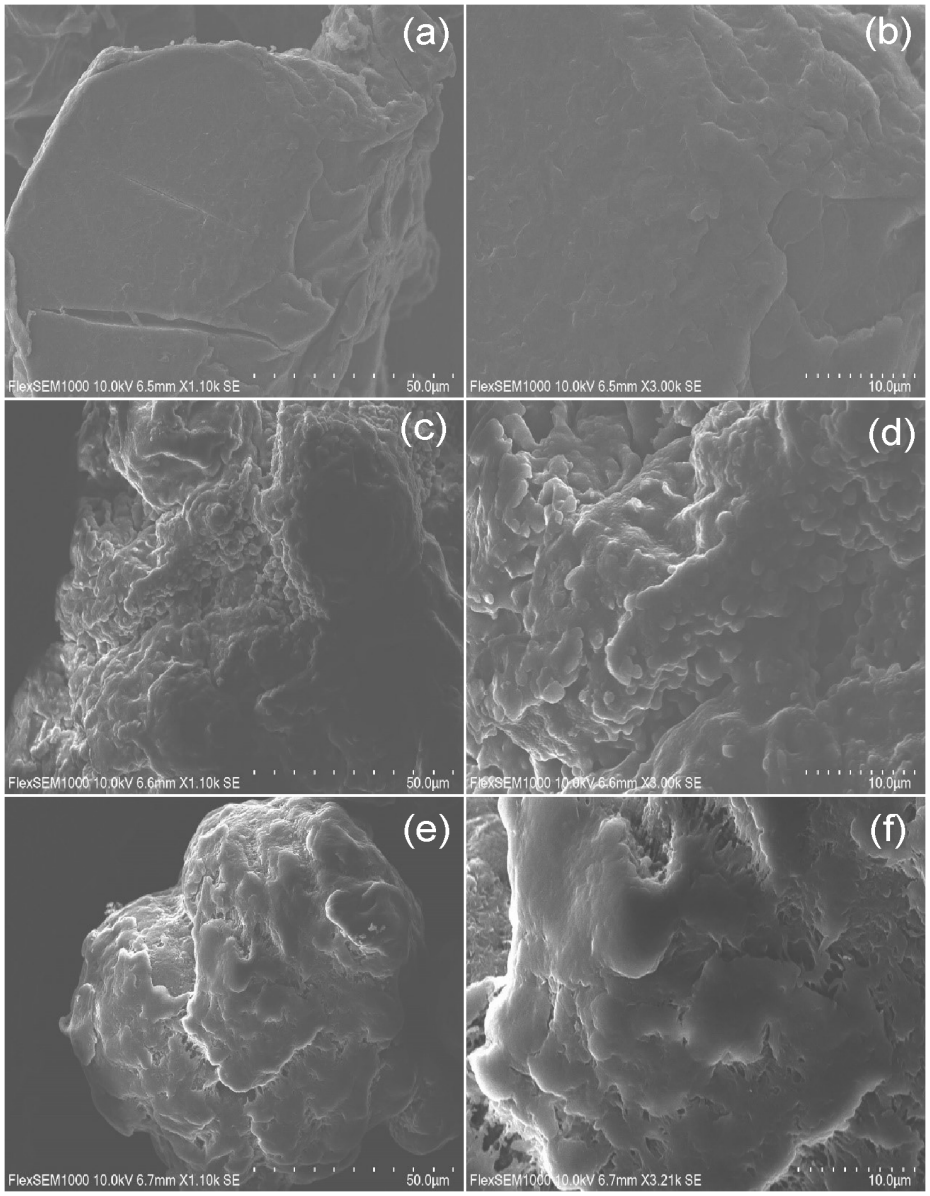

Figure 5. Scanning electron microscopy images of PS (**a**,**b**), PVC (**c**,**d**), and PE (**e**,**f**).

3.3.2. FTIR and XPS Analyses

Investigating the FTIR and XPS spectra of microplastics before and after antibiotic adsorption is essential for understanding the interaction mechanism between microplastics and antibiotics. As shown in Figure 6, after the adsorption of ENR and TMP onto the three types of microplastics, an O-H functional group appeared at 3440 cm^{-1}, suggesting that hydrogen bonding could be a possible mechanism during the adsorption process [38]. For PS, the skeletal vibration peak of C = C shifted from 1610 cm^{-1} to 1627 cm^{-1} after the adsorption of ENR, and from 1610 cm^{-1} to 1646 cm^{-1} after the adsorption of TMP, indicating that PS also adsorbed ENR and TMP through π–π conjugation [76], which explains why PS has a higher adsorption capacity. Additionally, a weak peak appeared at 1403 cm^{-1} after loading ENR onto microplastics, which could be attributed to the protonation and transfer of the pyrimidine group of ENR at 1387.15 cm^{-1}, indicating the presence of electrostatic attraction between ENR and the negatively charged surface of microplastics [77]. Furthermore, no new characteristic peaks were observed in the FTIR after the adsorption of antibiotics onto the microplastics, indicating that no new chemical bonds or functional groups were formed and the adsorption process was not a chemical process.

XPS spectra further confirmed the mechanism of ENR and TMP adsorption by microplastics. As shown in Figures S2–S4, the C 1s peaks of PS at 284.6 eV, 285.6 eV, and 291.3 eV were attributed to the aromatic carbon, C-H, and aromatic shake up, respectively [78]. The C 1s peaks of PVC at 284.6 eV and 286.0 eV were designated for C-C and C-Cl [79]. PE only contains C-C bonds at 284.8 eV [80]. After the adsorption of antibiotics by the microplastics, the N 1s and F 1s peaks of the N and F elements were observed in the XPS spectra of the microplastics, which proved that the antibiotics were successfully adsorbed to the surface, and the position of the C 1s peak did not move significantly, indicating that the chemical state of the C element did not change significantly and the adsorption was a physical adsorption process. After the adsorption of TMP by PS, the proportion of aromatic carbon increased, proving that the main mechanism of adsorption of ENR and TMP by PS was the π–π conjugation effect [45]. The increased C-Cl bond ratio after PVC's adsorption of ENR may be due to the electron donor provided by the Cl halogen atom, which promotes the adsorption of ENR on the PVC surface. Therefore, halogen bonds also have an important influence on the adsorption process [81]. Physical adsorption, possibly driven by π–π conjugation, halogen bonds, hydrogen bonds, and electrostatic interactions, was the main mechanism involved.

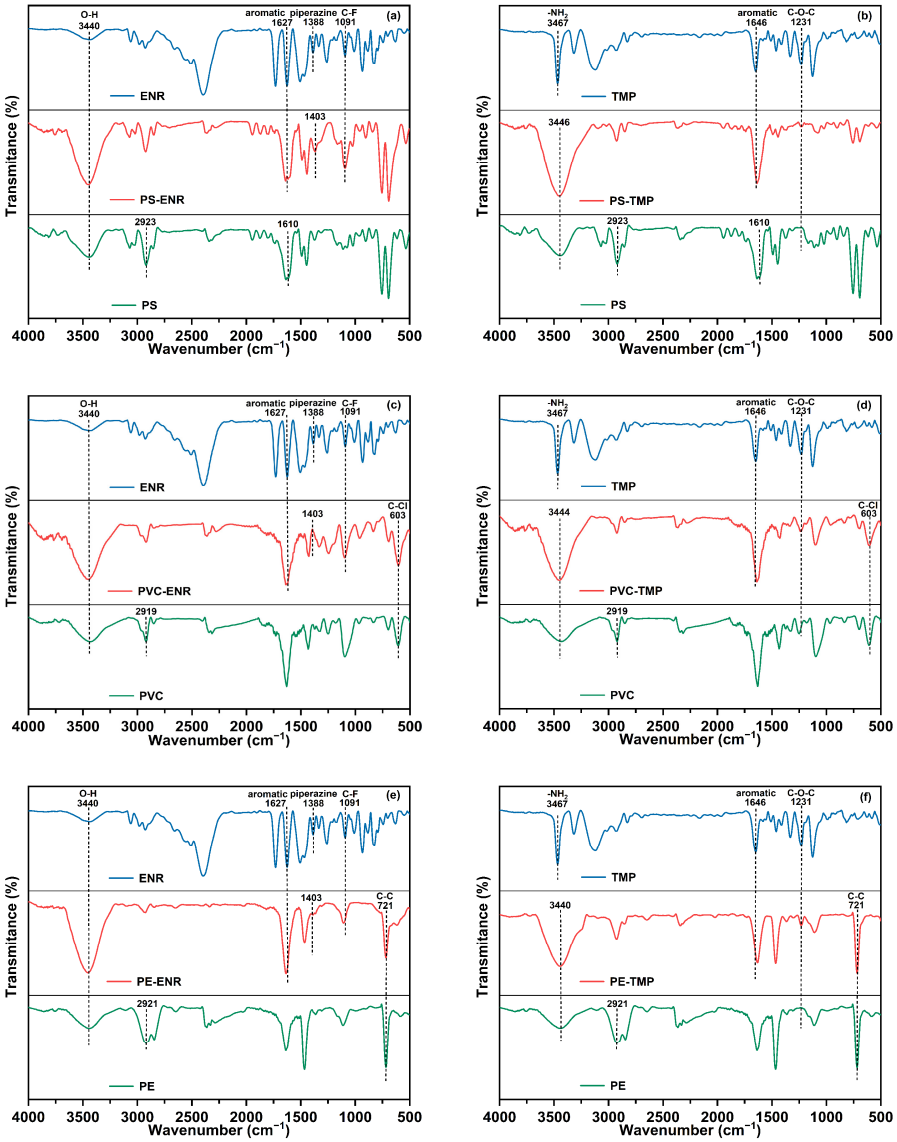

Figure 6. FTIR spectra of PS (**a**,**b**), PVC (**c**,**d**), and PE (**e**,**f**) before and after antibiotic adsorption.

3.4. Effects of Environmental Factors on Adsorption

3.4.1. pH

The influence of pH on the adsorption behavior of the microplastics is shown in Figure 7. When the pH increased, the adsorption capacity of the MPs increased first and then decreased. As for ENR, the adsorption capacity of the three types of microplastics reached its maximum at pH 7, and its capacity ranked as follows: PVC > PS > PE. However, for TMP, the maximum adsorption capacity occurred at pH 5, and the adsorption capacity ranked as follows: PS > PVC > PE.

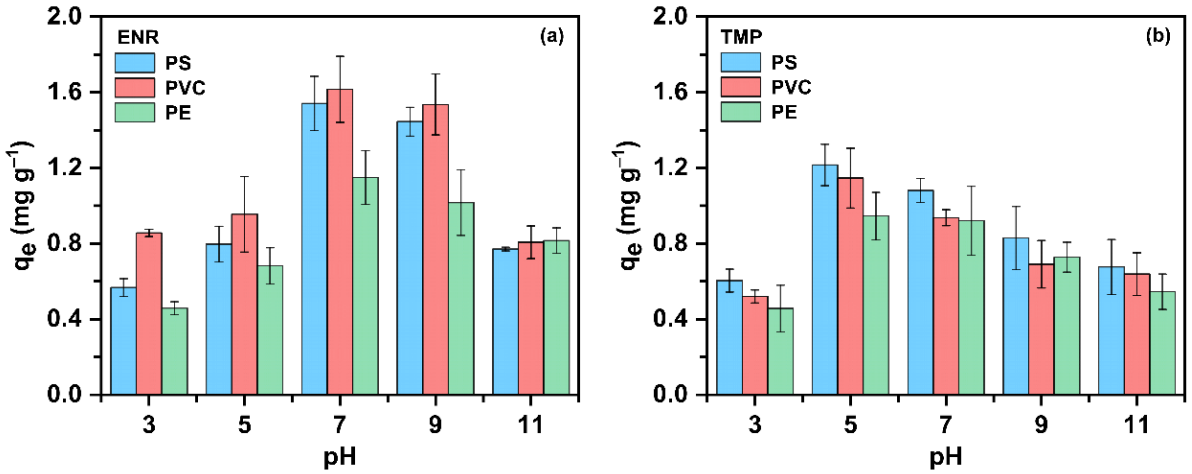

Figure 7. Effect of pH on adsorption of ENR (**a**) and TMP (**b**) by microplastics.

Zhang et al. (2020) found that, with the increase in pH, the adsorption of two quinolone antibiotics (LEV and NOR) on PS exhibited a trend of initially increasing and then decreasing, which was similar to our results [1]. The pK_a values for ENR are 6.2 and 7.6 and exist as zwitterions in solutions with pH between 6.2 and 7.6 [82]. With a pH < 5, the positively charged microplastics show electrostatic repulsion with cationic ENR; thus, the adsorption capacity is small and the concentration of H^+ in the solution is high, which produces competitive adsorption with the cationic ENR. With the increase in pH, the negatively charged microplastics exhibit electrostatic attraction with ENR and enhanced adsorption capacity, with the maximum adsorption capacity reached at pH 7.0. When the pH of the solution is greater than 7.0, the electrostatic repulsion between the negatively charged microplastics and the anionic ENR increases, and the adsorption capacity decreases. For TMP, the pK_a values of TMP are 3.2 and 6.8, and TMP exists as zwitterions in solutions with a pH between 3.2 and 6.8. With a pH < 3, the positive charged microplastics exhibit electrostatic repulsion with the cationic TMP, and the adsorption capacity is small. When the pH is 5, the negatively charged microplastics exhibit electrostatic attraction with the zwitterionic TMP, which enhances the adsorption capacity and reaches the maximum adsorption capacity.

3.4.2. Salinity

The effect of salinity on ENR and TMP on microplastics is shown in Figure 8. As the salinity gradually increased from 0 to 35‰, the adsorption capacity of the microplastics showed a negative correlation. When the salinity reached 35‰, the ENR and TMP adsorption capacity of the microplastics significantly decreased; the adsorption of PS, PVC, and PE for ENR decreased by 76.81%, 81.09%, and 80.76%, respectively, while the adsorption for TMP decreased by 59.33%, 51.65%, and 49.74%, respectively. These results indicate that salinity has a greater effect on the adsorption of ENR by microplastics compared to TMP.

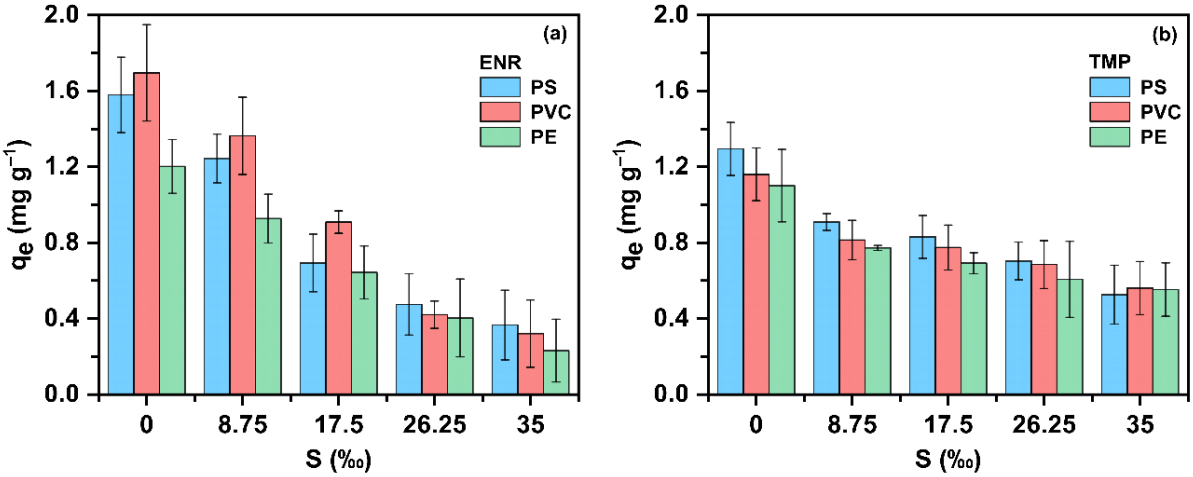

Figure 8. Effect of salinity on adsorption of ENR (**a**) and TMP (**b**) by microplastics.

High-salinity environments can affect the particle morphology of microplastics and antibiotic mass transfer. In a sodium chloride solution, microplastics aggregate to varying degrees, resulting in a smaller specific surface area, a reduction in adsorption sites on the surface, and an increase in repulsive forces between particles, thereby inhibiting the adsorption of antibiotics. At the same time, the microplastics under experimental conditions are in an anionic form, and the addition of Na^+ enhances the electrostatic attraction between Na^+ and microplastics, leading to competition for adsorption sites with antibiotics. The competition between adsorbents and electrolytes for electrostatic sites confirms the significant role of electrostatic interactions in the adsorption process [45]. As the salinity further increases, the influence of salinity on adsorption gradually levels off, because when the salinity reaches a certain level, the adsorption on the surface of the microplastics reaches equilibrium.

3.4.3. Aging

SEM images of aged microplastics are shown in Figure 9. After aging the microplastics, significant changes were observed in the physical morphology and chemical functional groups of the microplastics. Compared to the original microplastics (Figure 5), the surface of the aged microplastics becomes rougher, possibly due to the cracking and weathering caused by UV aging. Specifically, the cracks on the surface of aged PS increase, the protrusions on the surface of aged PVC become more pronounced, and obvious holes appear on the surface of aged PE. These changes greatly increase the specific surface area of microplastics and enhance their sensitivity to the penetration of antibiotic solutions [83].

The adsorption of antibiotics by aged microplastics is shown in Figure 10. The adsorption capacity of the three microplastics increased with the aging time: the ENR adsorption capacity of PS, PVC, and PE increased by 74.86%, 52.92%, and 60.46%, respectively. The TMP adsorption capacity of PS, PVC, and PE increased by 61.14%, 60.04%, and 65.24%, respectively. These results indicate that aged microplastics are more conducive to the adsorption of antibiotics.

Research has shown that the main reasons for the impact of aging on the adsorption performance of microplastics are the change in surface structure and the increase in hydrophilicity [84]. Fan et al. (2021) found that the aging of microplastics resulted in more pits and pores on the surface, increasing the specific surface area, which is beneficial for the binding of antibiotics [47]. Lee et al. (2014) found that the aging of microplastics leads to a decrease in crystallinity, which means a decrease in heat resistance and stiffness, making it

more favorable for the adsorption of pollutants [85]. Therefore, the aging of microplastics in the actual environment may enhance their carrier effect for organic pollutants.

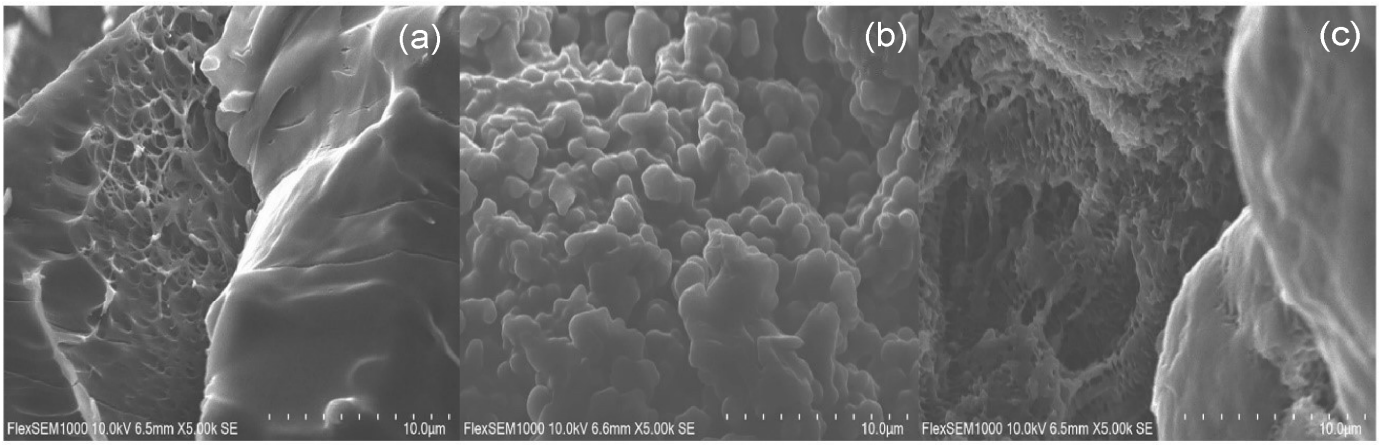

Figure 9. SEM images of PS (**a**), PVC (**b**), and PE (**c**) after aging.

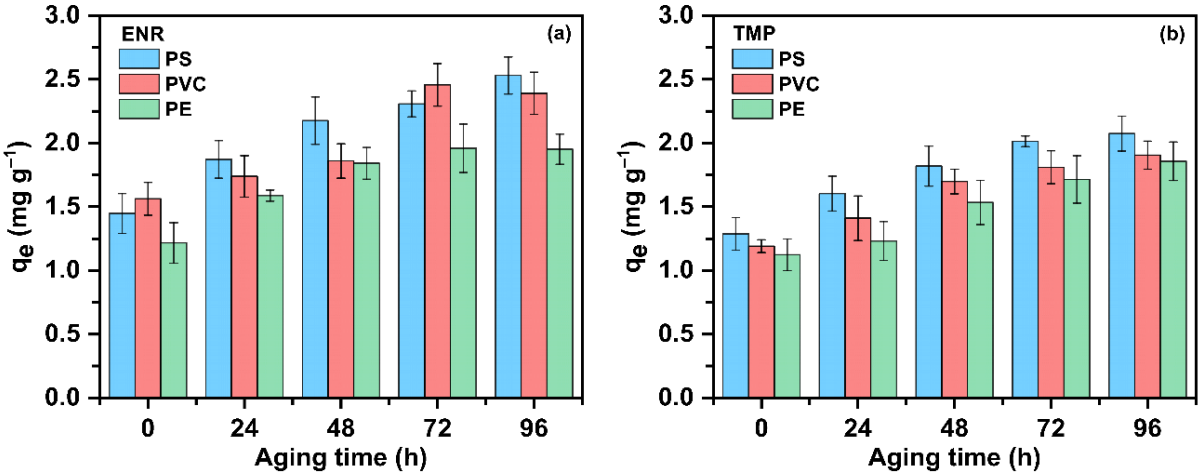

Figure 10. Effect of aging on adsorption of ENR (**a**) and TMP (**b**) on microplastics.

4. Conclusions

Microplastics can adsorb various antibiotics to varying degrees in the freshwater environment. The adsorption capacity of ENR (1.229~1.698 mg/g) was higher than that of TMP (1.110~1.306 mg/g), and the capacity was related to the log *Kow* of antibiotics. In addition, the adsorption capacity of PS and PVC for antibiotics is higher than that of PE, which is related to the specific surface area, polarity, and functional group of microplastics. The adsorption of antibiotics by microplastics followed pseudo-second-order kinetics and Freundlich isotherm models, indicating that the adsorption mode on their surfaces was non-uniform multilayer adsorption. In adsorption thermodynamics, the ΔH^0 ranges from 34.364 to 40.549 kJ/mol, and the ΔG^0 ranges from −17.603 to −11.270 kJ/mol, demonstrating that the process is spontaneous endothermic. The results of the spectral analysis show that the mechanism is physical adsorption, and the main mechanisms are π–π conjugation, halogen bonds, hydrogen bonding, and electrostatic interactions.

Desorption occurs when antibiotic-adsorbed microplastics enter a new environment. The desorption rates of ENR and TMP were 20.65% to 21.88% and 23.23% to 24.95%, respectively. In addition, the desorption rate of PE was higher than that of PS and PVC. The adsorption and desorption of antibiotics by microplastics can be affected by environmental factors.

The ENR and TMP adsorption capacity of the microplastics was the largest at pH 7 and 5, respectively. Salinity can significantly reduce the amount of antibiotics adsorbed by microplastics, up to 81.09%. Aging increases the adsorption of antibiotics by microplastics, up to 74.86%.

Antibiotics in natural environments often coexist; thus, when microplastics are present in environments containing multiple antibiotics, competitive antibiotic adsorption occurs. Therefore, future work should comprehensively consider other factors and investigate the adsorption and desorption of multiple coexisting antibiotics by microplastics in order to better contribute to the sustainable development goals.

Supplementary Materials: The following supporting information can be downloaded at: https://www.mdpi.com/article/10.3390/su17020516/s1, Figure S1: The XRD patterns of microplastics before and after adsorption of ENR and TMP; Figure S2: The XPS spectra of PS before and after adsorption of ENR and TMP; Figure S3: The XPS spectra of PVC before and after adsorption of ENR and TMP; Figure S4: The XPS spectra of PE before and after adsorption of ENR and TMP.

Author Contributions: Software, Z.L.; Validation, X.M.; Formal analysis, C.L.; Resources, X.M.; Data curation, Z.L. and C.Z.; Writing—original draft, Z.L. and C.L.; Visualization, X.S.; Supervision, X.S. and C.Z.; Project administration, C.Z.; Funding acquisition, C.Z. All authors have read and agreed to the published version of the manuscript.

Funding: This work was funded by the Key Technology and Application Project (2022YFC3106002) and the project of the Ministry of Natural Resources of the People's Republic of China (2019010AC).

Institutional Review Board Statement: Not applicable.

Informed Consent Statement: Not applicable.

Data Availability Statement: The original contributions presented in this study are included in the article/Supplementary Materials. Further inquiries can be directed to the corresponding authors.

Conflicts of Interest: The authors declare no conflict of interest.

Abbreviations

ENR	Enrofloxacin
TMP	Trimethoprim
PE	Polyethylene
PP	Polypropylene
PS	Polystyrene
PVC	Polyvinyl chloride
PA	Polyamide
PET	Polyethylene terephthalate
SEM	Scanning Electron Microscopy
BET	Brunauer–Emmett–Teller
FTIR	Fourier-Transform Infrared Spectroscopy
XRD	X-Ray Diffractometer
XPS	X-Ray Photoelectron Spectroscopy
HPLC	High-Performance Liquid Chromatography
PZC	Point of Zero Charge

References

1. Zhang, H.; Liu, F.F.; Wang, S.C.; Huang, T.Y.; Li, M.R.; Zhu, Z.L.; Liu, G.Z. Sorption of fluoroquinolones to nanoplastics as affected by surface functionalization and solution chemistry. *Environ. Pollut.* **2020**, *262*, 114347. [CrossRef]
2. Andrady, A.L. Microplastics in the marine environment. *Mar. Pollut. Bull.* **2011**, *62*, 1596–1605. [CrossRef] [PubMed]

3. Lambert, S.; Wagner, M. Characterisation of nanoplastics during the degradation of polystyrene. *Chemosphere* **2016**, *145*, 265–268. [CrossRef] [PubMed]
4. Bakir, A.; Rowland, S.J.; Thompson, R.C. Enhanced desorption of persistent organic pollutants from microplastics under simulated physiological conditions. *Environ. Pollut.* **2014**, *185*, 16–23. [CrossRef] [PubMed]
5. Abdurahman, A.; Li, S.; Li, Y.; Song, X.; Gao, R. Ecotoxicological effects of antibiotic adsorption behavior of microplastics and its management measures. *Environ. Sci. Pollut. Res.* **2023**, *30*, 125370–125387. [CrossRef] [PubMed]
6. Eriksen, M.; Lebreton, L.C.; Carson, H.S.; Thiel, M.; Moore, C.J.; Borerro, J.C.; Galgani, F.; Ryan, P.G.; Reisser, J. Plastic pollution in the world's oceans: More than 5 trillion plastic pieces weighing over 250,000 tons afloat at sea. *PLoS ONE* **2014**, *9*, e111913. [CrossRef] [PubMed]
7. Holmes, L.A.; Turner, A.; Thompson, R.C. Interactions between trace metals and plastic production pellets under estuarine conditions. *Mar. Chem.* **2014**, *167*, 25–32. [CrossRef]
8. Monteiro, R.C.; do Sul, J.A.I.; Costa, M.F. Plastic pollution in islands of the Atlantic Ocean. *Environ. Pollut.* **2018**, *238*, 103–110. [CrossRef]
9. Toumi, H.; Abidli, S.; Bejaoui, M. Microplastics in freshwater environment: The first evaluation in sediments from seven water streams surrounding the lagoon of Bizerte (Northern Tunisia). *Environ. Sci. Pollut. Res.* **2019**, *26*, 14673–14682. [CrossRef] [PubMed]
10. Barari, F.; Bonyadi, Z. Evaluation of the leaching of microplastics from discarded medical masks in aquatic environments: A case study of Mashhad city. *Appl. Water Sci.* **2023**, *13*, 229. [CrossRef]
11. Shirkhorshidi, B.; Ghanatghestani, M.D.; Moeinpour, F.; Parvaresh, H. The impacts of microplastics on sorption and desorption specifications of iron in soil. *Water Air Soil Pollut.* **2023**, *234*, 379. [CrossRef]
12. Li, C.; Busquets, R.; Campos, L.C. Assessment of microplastics in freshwater systems: A review. *Sci. Total Environ.* **2020**, *707*, 135578. [CrossRef] [PubMed]
13. Zhuang, S.; Wang, J. Interaction between antibiotics and microplastics: Recent advances and perspective. *Sci. Total Environ.* **2023**, *897*, 165414. [CrossRef] [PubMed]
14. Elizalde-Velázquez, A.; Carcano, A.M.; Crago, J.; Green, M.J.; Shah, S.A.; Cañas-Carrell, J.E. Translocation, trophic transfer, accumulation and depuration of polystyrene microplastics in Daphnia magna and *Pimephales promelas*. *Environ. Pollut.* **2020**, *259*, 113937. [CrossRef] [PubMed]
15. Zhang, X.; Tian, X.; Song, W.; Ma, B.; Chen, M.; Sun, Y.; Chen, Y.; Zhang, L. Adsorption of As (III) by microplastics coexisting with antibiotics. *Sci. Total Environ.* **2024**, *907*, 167857. [CrossRef]
16. Mato, Y.; Isobe, T.; Takada, H.; Kanehiro, H.; Ohtake, C.; Kaminuma, T. Plastic resin pellets as a transport medium for toxic chemicals in the marine environment. *Environ. Sci. Technol.* **2001**, *35*, 318–324. [CrossRef]
17. León, V.M.; García, I.; González, E.; Samper, R.; Fernández-González, V.; Muniategui-Lorenzo, S. Potential transfer of organic pollutants from littoral plastics debris to the marine environment. *Environ. Pollut.* **2018**, *236*, 442–453. [CrossRef]
18. Stapleton, M.J.; Ansari, A.J.; Hai, F.I. Antibiotic sorption onto microplastics in water: A critical review of the factors, mechanisms and implications. *Water Res.* **2023**, *233*, 119790. [CrossRef] [PubMed]
19. Wang, F.; Shih, K.M.; Li, X.Y. The partition behavior of perfluorooctanesulfonate (PFOS) and perfluorooctanesulfonamide (FOSA) on microplastics. *Chemosphere* **2015**, *119*, 841–847. [CrossRef] [PubMed]
20. Fu, L.; Li, J.; Wang, G.; Luan, Y.; Dai, W. Adsorption behavior of organic pollutants on microplastics. *Ecotoxicol. Environ. Saf.* **2021**, *217*, 112207. [CrossRef]
21. Liu, J.; Ma, Y.; Zhu, D.; Xia, T.; Qi, Y.; Yao, Y.; Guo, X.; Ji, R.; Chen, W. Polystyrene nanoplastics-enhanced contaminant transport: Role of irreversible adsorption in glassy polymeric domain. *Environ. Sci. Technol.* **2018**, *52*, 2677–2685. [CrossRef]
22. Brennecke, D.; Duarte, B.; Paiva, F.; Caçador, I.; Canning-Clode, J. Microplastics as vector for heavy metal contamination from the marine environment. *Estuar. Coast. Shelf Sci.* **2016**, *178*, 189–195. [CrossRef]
23. Velzeboer, I.; Kwadijk, C.; Koelmans, A. Strong sorption of PCBs to nanoplastics, microplastics, carbon nanotubes, and fullerenes. *Environ. Sci. Technol.* **2014**, *48*, 4869–4876. [CrossRef] [PubMed]
24. Hüffer, T.; Hofmann, T. Sorption of non-polar organic compounds by micro-sized plastic particles in aqueous solution. *Environ. Pollut.* **2016**, *214*, 194–201. [CrossRef] [PubMed]
25. Yang, Y.; Liu, W.; Xu, C.; Wei, B.; Wang, J. Antibiotic resistance genes in lakes from middle and lower reaches of the Yangtze River, China: Effect of land use and sediment characteristics. *Chemosphere* **2017**, *178*, 19–25. [CrossRef]
26. Klein, E.Y.; Van Boeckel, T.P.; Martinez, E.M.; Pant, S.; Gandra, S.; Levin, S.A.; Goossens, H.; Laxminarayan, R. Global increase and geographic convergence in antibiotic consumption between 2000 and 2015. *Proc. Natl. Acad. Sci. USA* **2018**, *115*, E3463–E3470. [CrossRef]
27. Du, Y.; Cheng, Q.; Qian, M.; Liu, Y.; Wang, F.; Ma, J.; Zhang, X.; Lin, H. Biodegradation of sulfametoxydiazine by Alcaligenes aquatillis FA: Performance, degradation pathways, and mechanisms. *J. Hazard. Mater.* **2023**, *452*, 131186. [CrossRef] [PubMed]

28. Lotfi Golsefidi, F.; Zahmatkesh Anbarani, M.; Bonyadi, Z. Removal of metronidazole antibiotic by modified red mud from aqueous solutions: Process modeling, kinetic, and isotherm studies. *Appl. Water Sci.* **2023**, *13*, 202. [CrossRef]
29. Kumar, R.R.; Lee, J.T.; Cho, J.Y. Fate, occurrence, and toxicity of veterinary antibiotics in environment. *J. Korean Soc. Appl. Biol. Chem.* **2012**, *55*, 701–709. [CrossRef]
30. Suzuki, S.; Hoa, P.T.P. Distribution of quinolones, sulfonamides, tetracyclines in aquatic environment and antibiotic resistance in Indochina. *Front. Microbiol.* **2012**, *3*, 67. [CrossRef] [PubMed]
31. Wang, Q.; Duan, Y.-J.; Wang, S.-P.; Wang, L.-T.; Hou, Z.-L.; Cui, Y.-X.; Hou, J.; Das, R.; Mao, D.-Q.; Luo, Y. Occurrence and distribution of clinical and veterinary antibiotics in the faeces of a Chinese population. *J. Hazard. Mater.* **2020**, *383*, 121129. [CrossRef]
32. Wang, B.; Xu, Z.; Dong, B. Occurrence, fate, and ecological risk of antibiotics in wastewater treatment plants in China: A review. *J. Hazard. Mater.* **2024**, 133925. [CrossRef] [PubMed]
33. Han, Q.; Zhao, S.; Zhang, X.; Wang, X.; Song, C.; Wang, S. Distribution, combined pollution and risk assessment of antibiotics in typical marine aquaculture farms surrounding the Yellow Sea, North China. *Environ. Int.* **2020**, *138*, 105551. [CrossRef] [PubMed]
34. Li, J.; Zhang, K.; Zhang, H. Adsorption of antibiotics on microplastics. *Environ. Pollut.* **2018**, *237*, 460–467. [CrossRef] [PubMed]
35. Yu, X.; Zhou, Z.-C.; Shuai, X.-Y.; Lin, Z.-J.; Liu, Z.; Zhou, J.-Y.; Lin, Y.-H.; Zeng, G.-S.; Ge, Z.-Y.; Chen, H. Microplastics exacerbate co-occurrence and horizontal transfer of antibiotic resistance genes. *J. Hazard. Mater.* **2023**, *451*, 131130. [CrossRef] [PubMed]
36. Lu, J.; Zhang, Y.; Wu, J.; Luo, Y. Effects of microplastics on distribution of antibiotic resistance genes in recirculating aquaculture system. *Ecotoxicol. Environ. Saf.* **2019**, *184*, 109631. [CrossRef]
37. Wu, X.; Xiao, B.; Li, R.; Wang, C.; Huang, J.; Wang, Z. Mechanisms and factors affecting sorption of microcystins onto natural sediments. *Environ. Sci. Technol.* **2011**, *45*, 2641–2647. [CrossRef] [PubMed]
38. Chen, Y.; Li, J.; Wang, F.; Yang, H.; Liu, L. Adsorption of tetracyclines onto polyethylene microplastics: A combined study of experiment and molecular dynamics simulation. *Chemosphere* **2021**, *265*, 129133. [CrossRef] [PubMed]
39. Armaković, S.J.; Armaković, S.; Savanović, M.M. Photocatalytic Application of Polymers in Removing Pharmaceuticals from Water: A Comprehensive Review. *Catalysts* **2024**, *14*, 447. [CrossRef]
40. Koelmans, A.A.; Besseling, E.; Wegner, A.; Foekema, E.M. Plastic as a carrier of POPs to aquatic organisms: A model analysis. *Environ. Sci. Technol.* **2013**, *47*, 7812–7820. [CrossRef] [PubMed]
41. Bour, A.; Haarr, A.; Keiter, S.; Hylland, K. Environmentally relevant microplastic exposure affects sediment-dwelling bivalves. *Environ. Pollut.* **2018**, *236*, 652–660. [CrossRef] [PubMed]
42. Chae, Y.; An, Y.-J. Effects of micro-and nanoplastics on aquatic ecosystems: Current research trends and perspectives. *Mar. Pollut. Bull.* **2017**, *124*, 624–632. [CrossRef]
43. Hall, N.; Berry, K.; Rintoul, L.; Hoogenboom, M. Microplastic ingestion by scleractinian corals. *Mar. Biol.* **2015**, *162*, 725–732. [CrossRef]
44. Wei, J.; Chen, M.; Wang, J. Insight into combined pollution of antibiotics and microplastics in aquatic and soil environment: Environmental behavior, interaction mechanism and associated impact of resistant genes. *TrAC Trends Anal. Chem.* **2023**, *166*, 117214. [CrossRef]
45. Guo, X.; Pang, J.; Chen, S.; Jia, H. Sorption properties of tylosin on four different microplastics. *Chemosphere* **2018**, *209*, 240–245. [CrossRef] [PubMed]
46. Ma, J.; Zhao, J.; Zhu, Z.; Li, L.; Yu, F. Effect of microplastic size on the adsorption behavior and mechanism of triclosan on polyvinyl chloride. *Environ. Pollut.* **2019**, *254*, 113104. [CrossRef]
47. Fan, X.; Gan, R.; Liu, J.; Xie, Y.; Xu, D.; Xiang, Y.; Su, J.; Teng, Z.; Hou, J. Adsorption and desorption behaviors of antibiotics by tire wear particles and polyethylene microplastics with or without aging processes. *Sci. Total Environ.* **2021**, *771*, 145451. [CrossRef]
48. Li, J.; Yu, S.; Chen, X.; Cai, Y.; Cui, M. Highly enhanced adsorption of antibiotics on aged polyamide microplastics. *Colloids Surf. A Physicochem. Eng. Asp.* **2023**, *658*, 130690. [CrossRef]
49. Al-Azzawi, M.S.; Knoop, O.; Drewes, J.E. Validation of sample preparation methods for small microplastics ($\leq$10 µm) in wastewater effluents. *Chem. Eng. J.* **2022**, *446*, 137082. [CrossRef]
50. Gillman, G.P.; Uehara, G. Charge characteristics of soils with variable and permanent charge minerals: II. Experimental. *Soil Sci. Soc. Am. J.* **1980**, *44*, 252–255. [CrossRef]
51. Gupta, V.K.; Rastogi, A.; Nayak, A. Biosorption of nickel onto treated alga (*Oedogonium hatei*): Application of isotherm and kinetic models. *J. Colloid Interface Sci.* **2010**, *342*, 533–539. [CrossRef] [PubMed]
52. Zahmatkesh Anbarani, M.; Najafpoor, A.; Barikbin, B.; Bonyadi, Z. Adsorption of tetracycline on polyvinyl chloride microplastics in aqueous environments. *Sci. Rep.* **2023**, *13*, 17989. [CrossRef]
53. Wang, C.; Fan, X.; Wang, P.; Hou, J.; Ao, Y.; Miao, L. Adsorption behavior of lead on aquatic sediments contaminated with cerium dioxide nanoparticles. *Environ. Pollut.* **2016**, *219*, 416–424. [CrossRef] [PubMed]
54. Wu, C.; Zhang, K.; Huang, X.; Liu, J. Sorption of pharmaceuticals and personal care products to polyethylene debris. *Environ. Sci. Pollut. Res.* **2016**, *23*, 8819–8826. [CrossRef] [PubMed]

55. Ying, G.-G.; Zhao, J.-L.; Zhou, L.-J.; Liu, S. Fate and occurrence of pharmaceuticals in the aquatic environment (surface water and sediment). In *Comprehensive Analytical Chemistry*; Elsevier: Amsterdam, The Netherlands, 2013; Volume 62, pp. 453–557.
56. Wu, B.; Taylor, C.M.; Knappe, D.R.; Nanny, M.A.; Barlaz, M.A. Factors controlling alkylbenzene sorption to municipal solid waste. *Environ. Sci. Technol.* **2001**, *35*, 4569–4576. [CrossRef]
57. Zu, B.; Li, W.; Lan, L.; Liu, Y.; Zhang, Y.; Li, J.; Mei, X. Adsorption of Tylosin and Tetracycline onto Microplastics: Behavior and Effects of Adsorbents and Salinity. *Water Air Soil Pollut.* **2023**, *234*, 582. [CrossRef]
58. Guo, X.; Liu, Y.; Wang, J. Sorption of sulfamethazine onto different types of microplastics: A combined experimental and molecular dynamics simulation study. *Mar. Pollut. Bull.* **2019**, *145*, 547–554. [CrossRef] [PubMed]
59. Wu, X.; Liu, P.; Huang, H.; Gao, S. Adsorption of triclosan onto different aged polypropylene microplastics: Critical effect of cations. *Sci. Total Environ.* **2020**, *717*, 137033. [CrossRef] [PubMed]
60. Sun, M.; Yang, Y.; Huang, M.; Fu, S.; Hao, Y.; Hu, S.; Lai, D.; Zhao, L. Adsorption behaviors and mechanisms of antibiotic norfloxacin on degradable and nondegradable microplastics. *Sci. Total Environ.* **2022**, *807*, 151042. [CrossRef] [PubMed]
61. Foo, K.Y.; Hameed, B.H. Insights into the modeling of adsorption isotherm systems. *Chem. Eng. J.* **2010**, *156*, 2–10. [CrossRef]
62. Razanajatovo, R.M.; Ding, J.; Zhang, S.; Jiang, H.; Zou, H. Sorption and desorption of selected pharmaceuticals by polyethylene microplastics. *Mar. Pollut. Bull.* **2018**, *136*, 516–523. [CrossRef] [PubMed]
63. Rangabhashiyam, S.; Anu, N.; Nandagopal, M.G.; Selvaraju, N. Relevance of isotherm models in biosorption of pollutants by agricultural byproducts. *J. Environ. Chem. Eng.* **2014**, *2*, 398–414. [CrossRef]
64. Ma, X.; Zhang, Z.; Wu, H.; Li, J.; Yang, L. Adsorption of volatile organic compounds at medium-high temperature conditions by activated carbons. *Energy Fuels* **2019**, *34*, 3679–3690. [CrossRef]
65. Wang, Z.; Yu, X.; Pan, B.; Xing, B. Norfloxacin sorption and its thermodynamics on surface-modified carbon nanotubes. *Environ. Sci. Technol.* **2010**, *44*, 978–984. [CrossRef] [PubMed]
66. Carter, M.C.; Kilduff, J.E.; Weber, W.J. Site energy distribution analysis of preloaded adsorbents. *Environ. Sci. Technol.* **1995**, *29*, 1773–1780. [CrossRef] [PubMed]
67. Li, H.; Zhang, D.; Han, X.; Xing, B. Adsorption of antibiotic ciprofloxacin on carbon nanotubes: pH dependence and thermodynamics. *Chemosphere* **2014**, *95*, 150–155. [CrossRef]
68. Ji, H.; Wan, S.; Liu, Z.; Xie, X.; Xiang, X.; Liao, L.; Zheng, W.; Fu, Z.; Liao, P.; Chen, R. Adsorption of antibiotics on microplastics (MPs) in aqueous environments: The impacts of aging and biofilms. *J. Environ. Chem. Eng.* **2024**, *12*, 111992. [CrossRef]
69. Pan, B.; Huang, P.; Wu, M.; Wang, Z.; Wang, P.; Jiao, X.; Xing, B. Physicochemical and sorption properties of thermally-treated sediments with high organic matter content. *Bioresour. Technol.* **2012**, *103*, 367–373. [CrossRef] [PubMed]
70. Xu, B.; Liu, F.; Cryder, Z.; Huang, D.; Lu, Z.; He, Y.; Wang, H.; Lu, Z.; Brookes, P.C.; Tang, C. Microplastics in the soil environment: Occurrence, risks, interactions and fate—A review. *Crit. Rev. Environ. Sci. Technol.* **2020**, *50*, 2175–2222. [CrossRef]
71. Zuo, L.-Z.; Li, H.-X.; Lin, L.; Sun, Y.-X.; Diao, Z.-H.; Liu, S.; Zhang, Z.-Y.; Xu, X.-R. Sorption and desorption of phenanthrene on biodegradable poly (butylene adipate co-terephtalate) microplastics. *Chemosphere* **2019**, *215*, 25–32. [CrossRef]
72. Cui, R.; Jong, M.-C.; You, L.; Mao, F.; Yao, D.; Gin, K.Y.-H.; He, Y. Size-dependent adsorption of waterborne Benzophenone-3 on microplastics and its desorption under simulated gastrointestinal conditions. *Chemosphere* **2022**, *286*, 131735. [CrossRef] [PubMed]
73. Guo, X.; Wang, X.; Zhou, X.; Kong, X.; Tao, S.; Xing, B. Sorption of four hydrophobic organic compounds by three chemically distinct polymers: Role of chemical and physical composition. *Environ. Sci. Technol.* **2012**, *46*, 7252–7259. [CrossRef]
74. Xu, B.; Liu, F.; Brookes, P.C.; Xu, J. The sorption kinetics and isotherms of sulfamethoxazole with polyethylene microplastics. *Mar. Pollut. Bull.* **2018**, *131*, 191–196. [CrossRef]
75. León, V.M.; García-Agüera, I.; Moltó, V.; Fernández-González, V.; Llorca-Pérez, L.; Andrade, J.M.; Muniategui-Lorenzo, S.; Campillo, J.A. PAHs, pesticides, personal care products and plastic additives in plastic debris from Spanish Mediterranean beaches. *Sci. Total Environ.* **2019**, *670*, 672–684. [CrossRef]
76. Xiong, Y.; Zhao, J.; Li, L.; Wang, Y.; Dai, X.; Yu, F.; Ma, J. Interfacial interaction between micro/nanoplastics and typical PPCPs and nanoplastics removal via electrosorption from an aqueous solution. *Water Res.* **2020**, *184*, 116100. [CrossRef] [PubMed]
77. Li, Z.; Hong, H.; Liao, L.; Ackley, C.J.; Schulz, L.A.; MacDonald, R.A.; Mihelich, A.L.; Emard, S.M. A mechanistic study of ciprofloxacin removal by kaolinite. *Colloids Surf. B Biointerfaces* **2011**, *88*, 339–344. [CrossRef] [PubMed]
78. Lin, Z.; Hu, Y.; Yuan, Y.; Hu, B.; Wang, B. Comparative analysis of kinetics and mechanisms for Pb (II) sorption onto three kinds of microplastics. *Ecotoxicol. Environ. Saf.* **2021**, *208*, 111451. [CrossRef] [PubMed]
79. Bigot, S.; Louarn, G.; Kébir, N.; Burel, F. Facile grafting of bioactive cellulose derivatives onto PVC surfaces. *Appl. Surf. Sci.* **2013**, *283*, 411–416. [CrossRef]
80. Louette, P.; Bodino, F.; Pireaux, J.-J. Poly (ethylene)(PE) XPS reference core level and energy loss spectra. *Surf. Sci. Spectra* **2005**, *12*, 49–53. [CrossRef]
81. Liu, Q.; Wu, H.; Chen, J.; Guo, B.; Zhao, X.; Lin, H.; Li, W.; Zhao, X.; Lv, S.; Huang, C. Adsorption mechanism of trace heavy metals on microplastics and simulating their effect on microalgae in river. *Environ. Res.* **2022**, *214*, 113777. [CrossRef] [PubMed]

82. Li, S.; Fang, L.; Ye, M.; Zhang, Y. Enhanced adsorption of norfloxacin on modified TiO_2 particles prepared via surface molecular imprinting technique. *Desalination Water Treat.* **2016**, *57*, 408–418. [CrossRef]
83. Ding, L.; Mao, R.; Ma, S.; Guo, X.; Zhu, L. High temperature depended on the ageing mechanism of microplastics under different environmental conditions and its effect on the distribution of organic pollutants. *Water Res.* **2020**, *174*, 115634. [CrossRef]
84. Mao, R.; Lang, M.; Yu, X.; Wu, R.; Yang, X.; Guo, X. Aging mechanism of microplastics with UV irradiation and its effects on the adsorption of heavy metals. *J. Hazard. Mater.* **2020**, *393*, 122515. [CrossRef] [PubMed]
85. Lee, H.; Shim, W.J.; Kwon, J.-H. Sorption capacity of plastic debris for hydrophobic organic chemicals. *Sci. Total Environ.* **2014**, *470*, 1545–1552. [CrossRef] [PubMed]